Improved activity standardization of $^{90}Sr/^{90}Y$ by means of liquid scintillation counting

Karsten Kossert, Xavier Mougeot

Improved activity standardization of $^{90}Sr/^{90}Y$ by means of liquid scintillation counting

Karsten Kossert[*1], Xavier Mougeot[2]

[1] *Physikalisch-Technische Bundesanstalt (PTB), Bundesallee 100, 38116 Braunschweig, Germany*

[2] *CEA, LIST, Laboratoire National Henri Becquerel, F-91191 Gif-sur-Yvette, France*

Abstract

Radioactive strontium isotopes play an important role in environmental radioactivity. Reliable activity standards are required in order to validate radioanalytical techniques and related measurements. In this paper, improved methods for the primary activity standardization of $^{90}Sr/^{90}Y$ based on liquid scintillation counting are presented. To this end, two methods were used: the CIEMAT/NIST efficiency tracing technique with ^{3}H as a tracer and the triple-to-double coincidence ratio method. Non-negligible discrepancies between the two methods were found when applying existing analysis techniques. A detailed study was carried out to identify and eliminate the root causes of these discrepancies.

Eventually, excellent agreement between the two methods was obtained. This required advanced beta spectrum calculations which were carried out with a specific version of the BetaShape program taking the atomic exchange effect into account. In addition, it was found that the quench-indicating parameters determined in commercial liquid scintillation counters are biased, which can cause significant problems for the CIEMAT/NIST efficiency tracing method. The effect depends on the counting rate and can be explained by a superposition of the LS spectra generated by $^{90}Sr/^{90}Y$ and the external standard source.

Key words: $^{90}Sr/^{90}Y$; activity standardization; beta spectrum shapes; liquid scintillation counting

* Corresponding author:
e-mail address: Karsten.Kossert@ptb.de

1. Introduction

In radionuclide metrology, the activity standardization of pure beta emitting radionuclides is often done by means of liquid scintillation (LS) counting, and the two most frequently used methods are the triple-to-double coincidence ratio (TDCR) technique and the CIEMAT/NIST efficiency tracing (CNET) method (Broda et al., 2007). Both methods are based on the same free-parameter model (Grau Malonda, 1999). When carrying out an activity standardization of a given beta emitting radionuclide, it is expected that:

i) The results of both methods agree within the uncertainties.

ii) The results obtained with the same method are consistent when varying the counting efficiency within certain limits.

It was, indeed, found that both expectations are met when standardizing several radionuclides, though small deviations have been observed in some cases (see, e.g., Nähle and Kossert, 2011). However, for some radionuclides, significant trends were observed when varying the counting efficiency, and/or the results of the TDCR method and the CNET technique were not in agreement. Such inconsistencies must be regarded as an indication that the model and/or the measurements were imperfect. When considering the model, some studies focused on the ionization quenching function $Q(E)$ (e.g., Broda et al., 2002) or the statistical model (Broda and Jęczmieniowski, 2004; Bobin et al., 2012). Another potential reason for discrepancies could be inaccurate nuclear decay data, which are required as input data for the efficiency computation. For beta emitters, the relevant decay data comprise the maximum beta energy and the shape of the beta spectrum. An interesting example is ^{63}Ni, a pure beta emitter which has a maximum energy of only 66.980(15) keV (Bé et al., 2006). For this radionuclide, it was shown that discrepancies between the LS methods could only be resolved when using advanced beta spectrum calculations that precisely include the atomic exchange and screening effects (Kossert and Mougeot, 2015). Since the study on ^{63}Ni, several further systematic studies with other radionuclides have been carried out, and it was found that deviations –

which are sometimes rather small – are reduced when using improved beta spectra. In this work, a study on ^{90}Sr in radioactive equilibrium with its daughter ^{90}Y is presented. Since both radionuclides have rather high maximum beta energies, the overall LS counting efficiency is also rather high and little influence of the beta spectrum shapes is expected. Thanks to advanced measurement and analysis techniques it can, however, be shown that – even in this case – the more advanced beta spectrum calculations reduce the deviations. Moreover, it was found that the determination of the quench-indicating parameter can be biased when using commercial LS counters. Accurate results are obtained only when correcting for this effect. The work presented here is relevant to ensuring the availability of reliable and reproducible activity standards for ^{90}Sr/^{90}Y with low uncertainty. Strontium-90 plays an important role in industry and medicine, and it is a source for ^{90}Y which – in turn – is widely applied in nuclear medicine for palliative treatments and cancer therapy. Since ^{90}Sr is a nuclear fission product, it is of concern in fallout from nuclear weapons and nuclear accidents. Consequently, it is one of the most relevant radionuclides in environmental radioactivity, and accurate activity standards help to establish corresponding measurements and analysis techniques (see, e.g., Bruchertseifer et al., 2008).

2. LS efficiency calculation

Strontium-90 ($T_{1/2}$=28.80(7) a) decays by beta minus transition with a maximum beta energy of 545.9 keV to the shorter-lived beta emitter ^{90}Y ($T_{1/2}$=2.6684(13) d), which has a rather high maximum beta energy of 2278.7 keV. In this work, the transition probability of the latter beta transition was assumed to be 100%, since two other weak beta-gamma transitions were neglected. The transition energy of ^{90}Y is high enough to make internal pair production possible (Selwyn et al., 2007), and recent studies confirm that the corresponding probability is only about 3.2 10^{-5} (Pibida et al., 2020; Dryák and Šolc, 2020). Therefore, this effect was also

neglected in this work. Nuclear decay data – as stated above – were taken from Bé et al. (2006).

The beta transitions of ^{90}Sr and ^{90}Y are both of a unique 1st forbidden nature. In this work, the corresponding beta spectra were calculated with a new version of the BetaShape program, taking the atomic exchange and screening effects into account. Compared to the modelling of the available version of the code (Mougeot, 2017), different improvements were added. The screening effect is precisely taken into account by the full numerical solving of the Dirac equation for a Coulomb potential of the nucleus that includes screened potentials (Mougeot and Bisch, 2014). The exchange effect has been improved by adding the contribution of the $p_{1/2}$ orbitals and by considering more precise atomic energies, as described in (Hayen et al., 2018) – only $s_{1/2}$ orbitals and less precise atomic energies were considered in (Mougeot and Bisch, 2014). The radiative corrections are now those considered in the high-precision study of superallowed beta decays (Towner and Hardy, 2008; Czarnecki et al., 2004). The program also provides a spectrum which ignores the above-mentioned effects. In the following, this latter spectrum is referred to as the "classical" beta spectrum. In several analysis codes which were used for LS counting in the past (see, e.g., Garcia-Toraño and Grau Malonda, 1985; Broda et al.., 2000) a shape-factor function $C(W)=q^2+p^2$ was used. In the following, this is referred to as the "old approximation".

Figure 1 shows the calculated beta spectra of ^{90}Sr (top), ^{90}Y (middle), and ^{90}Sr in radioactive equilibrium with ^{90}Y (bottom). For the latter spectrum, the individual spectra were first normalized. The ^{90}Y spectrum was then multiplied by the equilibrium factor $\frac{T_{1/2}(^{90}\mathrm{Sr})}{T_{1/2}(^{90}\mathrm{Sr})-T_{1/2}(^{90}\mathrm{Y})}=1.000254$ before adding both spectra. In the case of the more advanced beta spectrum calculations, the probability of emitting low-energy beta electrons is slightly higher, which is mainly due to the atomic exchange effect.

The LS counting efficiencies were calculated in a similar manner to that described by Nähle and Kossert (2011): the ionization quenching function was calculated applying the methodology of the KB code (Los Arcos and Ortiz, 1997) and the atomic composition of the samples was taken into account. When applying the CNET method, the efficiency computations for ^{3}H and $^{90}Sr/^{90}Y$ were carried out with the same value for the *kB* parameter, which was selected to be 0.0075 cm/MeV.

3. Experimental details

The solution used for this study contains ^{90}Sr as $SrCl_2$. The composition is similar to that described by Kossert and Nähle (2015) with an $SrCl_2 \cdot 6H_2O$ concentration of 50 mgL^{-1} and a $YCl_3 \cdot 6H_2O$ concentration of 46 mgL^{-1} in 0.1 M HCl. The nominal activity concentration is about 4 kBq/g, and no radioactive impurity could be detected by means of gamma-ray spectrometry.

The LS samples were prepared with 15 mL Ultima Gold™ LS cocktail using 20 mL glass vials from PerkinElmer. About 1 mL of distilled water was added to one sample that was then used to measure the background counting rates. Three additional samples were prepared adding about 0.6 mL of distilled water to each of them and small amounts of nitromethane to two of them. Finally, weighed portions of about 400 mg of the radioactive solution were added. The sample compositions are summarized in Table 1.

The LS measurements were carried out in a custom-built TDCR counter at PTB referred to as TDCR-M29. The system makes use of an FPGA-based coincidence module (Nähle et al., 2014) which employs the dead time and the coincidence logic of the MAC3 module (Bouchard and Cassette, 2000), i.e. it is also a live-timed system with extendable dead time. In this work, a coincidence resolving time of 40 ns was used. The inner part of the optical chamber is made of the diffuse reflecting material *OP.DI.MA* (ODM98), produced by

Gigahertz Optik GmbH, which holds three Hamamatsu R331-05 photomultiplier tubes (PMTs). The discriminator thresholds were adjusted just below the single electron peak. An additional feature of TDCR-M29 is an automated sample changer which is very useful, in particular when carrying out many measurements over a long time (Kossert and Nähle, 2015).

In addition, two commercial LS counters were used. A Wallac 1414 Guardian^{TM} liquid scintillation spectrometer was used to apply the CNET method. A measured LS spectrum of this instrument is shown in Fig. 2 (left). A TriCarb2800 TR from PerkinElmer was also used to obtain an LS spectrum (Fig. 2, right). However, the application of the CNET method with experimental data from this counter was omitted as explained in the following section.

4. Analysis and results

The experimental data were analysed as described in previous articles (see, e.g., Nähle and Kossert, 2011) with corrections for background, decay and decay during the measurement.

In the course of a preliminary analysis, small deviations between the results of the CNET and the TDCR methods were found. Further similar ^{90}Sr measurements at PTB indicate comparable deviations. These deviations were slightly larger when using higher ^{90}Sr activities (higher counting rates) in the LS samples and lower when measuring lower activities. Eventually, a closer look revealed a bias of the quench-indicating parameter $SQP(E)$ as determined in the Wallac counter. At PTB, the experimentally determined $SQP(E)$ value is used to determine a related ^{3}H efficiency from a calibration curve. This calibration curve, i.e. the function ^{3}H efficiency vs $SQP(E)$, is obtained from an independent measurement of a ^{3}H activity standard solution (tritiated water) with a similar composition to the LS samples of the nuclide under study.

When preparing LS samples at PTB, the composition of the background sample (No. 1) is usually very similar to the composition of one of the radioactive samples (No. 2) which does not contain any nitromethane (cf. Table 1). Therefore, similar results for the quench-indicating parameter are expected. In the case of ^{90}Sr, this was, however, not so. The measured quench-indicating parameter $SQP(E)$ of the ^{90}Sr sample was found to be significantly larger than the $SQP(E)$ of the background sample. In the following, the bias is defined as $\Delta SQP(E) = SQP(E)_{\text{Sr-90}} - SQP(E)_{\text{background}}$, with $SQP(E)_{\text{Sr-90}}$ and $SQP(E)_{\text{background}}$ being the measured quench-indicating parameters of the unquenched ^{90}Sr LS sample (No. 2) and the background sample, respectively.

A systematic analysis of several LS measurement data collected at PTB over a number of years indicates that this bias is correlated with the net counting rate of the unquenched ^{90}Sr sample, i.e. a higher net counting rate leads to a higher bias. In commercial LS counters, the quench-indicating parameter is automatically determined from the LS spectrum created due to irradiation with an external gamma-ray emitting source, referred to as the external standard ($SQP(E)$ = Spectral Quench Parameter of the External standard). In the Wallac counter, the external standard corresponds to a ^{152}Eu source, and the system applies an algorithm to the measured spectrum (see, e.g., Grau Malonda, 1999). A prerequisite of the CNET method is that this quench-indicating parameter does not depend on the radionuclide in the LS sample and it should also not depend on the counting rate. Apparently, these requirements are not fulfilled in the case of ^{90}Sr, which might be due to an overlap of the spectrum created by ^{90}Sr/^{90}Y and the spectrum due to the detection of radiation originating from the ^{152}Eu source. The effect could be eliminated when measuring the LS spectrum of the ^{90}Sr/^{90}Y LS sample and subtracting it from the LS spectrum obtained when measuring the LS sample plus the external source (after normalization of both spectra). When assuming that no such subtraction is performed by the commercial counter system, it is expected that the bias also depends on

the activity of the external standard source. Figure 3 shows the bias as a function of the net counting rate divided by the activity of the external standard source. It is noteworthy that the data used for Fig. 3 were obtained in a period of about 12 years. Therefore, the activity of the external ^{152}Eu standard ($T_{1/2}$≈13.5 a) changed significantly. Interestingly, Fig. 3 shows an almost linear correlation.

A similar study was carried out with measurement data from the TriCarb counter, which contains a ^{133}Ba ($T_{1/2}$≈10.5 a) source as an external standard. Here, the quench-indicating parameter is the *tSIE* (transformed Spectra Index of the External standard), and a similar bias was found (see Fig. 3, right).

For the Wallac measurements described in this work, the bias was found to be $\Delta SQP(E) = 6$ which corresponds to about 0.77% of the measured value ($SQP(E)$=780). After correction, the ^{90}Sr/^{90}Y activity increases by about 0.06%. It was assumed that all samples are affected by the same bias $\Delta SQP(E)$.

In the TriCarb, the bias was found to be $\Delta tSIE = 10$ which corresponds to about 1.9% of the measured value (*tSIE*=472). After correction, the ^{90}Sr/^{90}Y activity increases by about 0.05%, i.e. the effects in both counters are very similar. The final results from the TriCarb are about 0.13% lower than those of the Wallac counter. Similar small deviations between the two counters were found for other radionuclides and are assigned to potential imperfect signal treatment in the TriCarb that is not discussed in this article. In the following, the TriCarb data are omitted.

The background sample (cf. Table 1) does not contain any carrier solution, and consequently, its composition differs slightly from that of sample No. 2. One may wonder whether this difference could also cause a bias for the quench-indicating parameter. Therefore, a further background sample was prepared using 15 mL Ultima Gold, 0.6 mL of distilled water and

400 mg of a corresponding carrier solution as described in Section 3. The quench-indicating parameter of the new background sample was found to be slightly lower in both commercial LS counters, but the differences were not significant.

Figure 4 shows the results of the activity analyses under various conditions. In a first step, the data were analysed using the "old approximation" with $C(W)=q^2+p^2$. In this case, the CNET results (crosses) show a little trend and the unweighted mean is about 0.26% lower than the unweighted mean of the corresponding TDCR results (open circles). When using the classical beta spectrum, the CNET results (open diamonds) still show a slight trend and the unweighted mean is about 0.16% lower than the unweighted mean of the corresponding TDCR results (open squares). The unweighted mean values are also shown in Table 2. The deviation between the two methods is reduced to less than 0.1% when the CNET results are corrected for the $SQP(E)$ bias (open triangles).

When using the more advanced beta spectrum calculations that include atomic-exchange and screening effects, the results of both methods (blue, filled symbols in Fig. 4) increase slightly, and the relative deviation between the methods is reduced to be less than 0.04%. When considering the uncertainties, this deviation can be considered as not significant.

Table 2 includes results obtained when using a modified Birks parameter kB = 0.0110 cm/MeV. When using this value, the deviation between the two methods increases to about 0.18%, even if the quench-indicating parameter correction is applied and the new beta spectra are used. Interestingly, the mean value of both methods is very similar to the final result which is based on kB = 0.0075 cm/MeV. This shows that the application of both methods is advantageous, since the mean value is often very robust to changes of the kB parameter. A similar anti-correlation was found in previous works (see, e.g., Nähle and Kossert, 2011; Kossert and Mougeot, 2015; Kossert et al., 2018).

Uncertainties were conservatively estimated according to common practice in radionuclide metrology (Kossert et al., 2015), and corresponding uncertainty budgets for both methods are shown in Table 3. The unweighted mean value a = 3.981(6) kBq/g (cf. Table 2) is taken as the final result. Since the results of the two methods are correlated, e.g., due to the beta spectrum and due to the weighing procedures, the relative uncertainty is conservatively estimated to be 0.14%, which corresponds to the relative standard uncertainty of the TDCR method.

5. Conclusions and discussion

The work presented here again reveals that commercial LS counters are imperfect. In previous articles and conference papers, the importance of threshold adjustments, correct dead-time treatment and the accurate determination of the starting time of a measurement were emphasized, and problems due to certain features (like the delay before burst counting in TriCarb counters) were criticized (Cassette, 2017; Kossert and Nähle, 2011). Here, the list of problematic aspects is extended, since the determination of the quench-indicating parameter is – in some cases – also not reliable.

One potential solution to this problem could be to prepare composition-matched sources for ^{3}H and the nuclide under study when applying the CNET method. Such an approach has often been applied at NIST (see, e.g., Collé et al., 2008) and good results have been obtained. The approach requires some expertise concerning sample preparation and also has some drawbacks. For instance, it reduces the flexibility of the method and, in some cases, it is difficult or even impossible to prepare appropriate matched sources. Another solution could be to build a CNET counter rather than to buy a commercial system. This would ensure full control over all relevant parameters including PMT discriminator thresholds, and a live-time-based extendable dead

time could be used. At present, the radioactivity group at PTB plans to build its own CNET counter, which is to comprise an external standard to measure a quench-indicating parameter.

A further important conclusion is that accurate beta spectra calculations are essential to reduce (or even eliminate) discrepancies between the results from the CNET and the TDCR methods. For the high-energy beta emitter ^{90}Sr/^{90}Y, the changes are lower than for ^{63}Ni (Kossert and Mougeot, 2015) or ^{60}Co (Kossert et al., 2018) but still clearly visible.

The analysis presented here can also be regarded as a validation of new beta spectra calculations and – as already mentioned – we have similar findings for several other beta emitting radionuclides, and a comprehensive review article is planned.

Despite the significant progress made for allowed and unique forbidden beta transitions, the computation of beta spectra of non-unique forbidden transitions is still challenging. For this type of transition, the nuclear structure must be taken into account, and to date, there is still no full model with related computation tools. For the development of such a model, it is essential to have access to reliable experimental data, which must include precise measurements of the low-energy part of the beta spectra. It has been demonstrated in several works that metallic magnetic calorimeters (MMCs) are excellent tools for this task (Rotzinger et al., 2008; Loidl et al., 2010, 2014, 2019). MMCs are a special type of low-temperature detector which provides a high energy resolution, high linearity and a low energy threshold when carrying out 4π measurements of beta emitting radionuclides. The experimentally determined beta spectra can also be used directly for the analysis of LS counting data or to apply the TDCR-Čerenkov method (Kossert, 2010; Kossert et al., 2014). In this way, considerable improvements were achieved for ^{241}Pu (Kossert et al., 2011a) and ^{36}Cl (Kossert et al., 2011b), and preliminary results for ^{99}Tc look promising.

The authors, therefore, emphasize that further improvements of beta spectrum calculations and corresponding high-precision measurements are needed and that it is extremely important for

the required research to receive sufficient support from the nuclear physics community and funding bodies.

References

Bé, M.-M., Chisté, V., Dulieu, C., Browne, E., Baglin, C., Chechev, V., Kuzmenco, N., Helmer, R., Kondev, F., MacMahon, D., Lee, K.B., 2006. Table of radionuclides. Monographie BIPM-5 Vol. 3, Bureau International des Poids et Mesures, Sèvres.

Bobin C., Thiam, C., Chauvenet, B., Bouchard, J., 2012. On the stochastic dependence between photomultipliers in the TDCR method. Appl. Radiat. Isot. 70, 770-780.

Bouchard, J., Cassette, P., 2000. MAC3: an electronic module for the processing of pulses delivered by a three photomultiplier liquid scintillation counting system. Appl. Radiat. Isot. 52, 669-672.

Broda, R., Cassette, P., Małetka, K., Pochwalski, K., 2000. A simple computing program for application of the TDCR method to standardization of pure-beta emitters. Appl. Radiat. Isot. 52, 673-678.

Broda, R., Małetka, K., Terlikowska, T., Cassette, P., 2002. Study of the influence of the LS-cocktail composition for the standardisation of radionuclides using the TDCR model. Appl. Radiat. Isot. 56, 285-289.

Broda, R., Jęczmieniowski, A., 2004. Statistics of the LS-detector in the case of low counting efficiency. Appl. Radiat. Isot. 60, 453-458.

Broda, R., Cassette, P., Kossert, K., 2007. Radionuclide Metrology using liquid scintillation counting. Metrologia 44, S36-S52.

Bruchertseifer, F., Eikenberg, J., Frenzel, E., Frenzel, S., Geering, J.-J., Gerstmann, U., Happel, S., Krause, W.J., Speer, W., Steinkopff, Th., Tait, D., Vetter, A., Wershofen, H., 2008. Moderne Routine- und Schnellmethoden zur Bestimmung von Sr-89 und Sr-90 bei der

Umweltüberwachung. Fortschritte im Strahlenschutz, Fachverband für Strahlenschutz e.V. (Ed.), FS-08-147-AKU, ISSN 1013-4506, ISBN 978-38249-1119-6, TÜV Media GmbH Cologne.

Cassette Ph., 2017. "With a little bit of effort, manufacturers could make better LS counters, even suitable for radionuclide metrology". Lecture given at the "LSC2017 – Advances in Liquid Scintillation Spectrometry" conference, 1-5 May 2017, Copenhagen Denmark, http://lsc2017.nutech.dtu.dk/wp-content/uploads/2-Cassette-lsc2017-203.pdf (website accessed March 2020).

Collé, R., Zimmerman, B.E., Cassette, P., Laureano-Perez, L., 2008. ^{63}Ni, its half-life and standardization: Revisited. Appl. Radiat. Isot. 66, 60-68.

Czarnecki, A., Marciano, W.J., Sirlin, A., 2004. Precision measurements and CKM unitarity. Phys. Rev. D 70, 093006.

Dryák, P. Šolc, J., 2020. Measurement of the branching ratio related to the internal pair production of Y-90. Appl. Radiat. Isot. 156, 108942.

Garcia-Toraño, E., Grau Malonda, A., 1985. EFFY, a new program to compute the counting efficiency of beta particles in liquid scintillators. Comput. Phys. Comm. 36, 307-312.

Grau Malonda, A., 1999. Free parameter models in liquid scintillation counting. Colección Documentos CIEMAT. CIEMAT, ISBN 84-7834-350-4.

Hayen, L., Severijns, N., Bodek, K., Rozpedzik, D., Mougeot, X., 2018. High precision analytical description of the allowed β spectrum shape. Rev. Mod. Phys. 90 (1), 015008.

Kossert, K., 2010. Activity standardization by means of a new TDCR-Čerenkov counting technique. Appl. Radiat. Isot. 68, 1116-1120.

Kossert, K., Nähle, O., 2011. Activity determination of ^{228}Th by means of liquid scintillation counting. LSC2010, Advances in Liquid Scintillation Spectrometry: Proceedings of the 2010 International Conference on Liquid Scintillation Spectrometry, Paris, France, 6-10

September 2010, edited by Philippe Cassette, in Radiocarbon, the University of Arizona, Tucson, Arizona, USA, 2011, ISBN 978-0-9638314-7-7, 151-160.

Kossert, K., Nähle, O., Grau Carles, A., 2011a. Beta shape-factor function and activity determination of ^{241}Pu. Appl. Radiat. Isot. 69, 1246-1250.

Kossert, K., Grau Carles, A., Nähle, O., 2011: Čerenkov counting and liquid scintillation counting of ^{36}Cl. LSC2010, Advances in Liquid Scintillation Spectrometry: Proceedings of the 2010 International Conference on Liquid Scintillation Spectrometry, Paris, France, 6-10 September 2010, edited by Philippe Cassette, in Radiocarbon, the University of Arizona, Tucson, Arizona, USA, 2011, ISBN 978-0-9638314-7-7, 161-170.

Kossert, K., Grau Carles, A., Nähle, O.J., 2014. Improved Čerenkov counting techniques based on a free-parameter model. Appl. Radiat. Isot. 86, 7-12.

Kossert, K., Nähle, O.J., 2015. Disproof of solar influence on the decay rates of ^{90}Sr/^{90}Y. Astropart. Phys. 69, 18-23.

Kossert, K., Broda, R., Cassette, Ph., Ratel, G., Zimmerman, B., 2015. Uncertainty determination for activity measurements by means of the TDCR method and the CIEMAT/NIST efficiency tracing technique. Metrologia 52, S172-S190 (Special Issue on Uncertainty Evaluation in Radionuclide Metrology).

Kossert, K., Mougeot, X., 2015. The importance of the beta spectrum calculation for accurate activity determination of ^{63}Ni by means of liquid scintillation counting. Appl. Radiat. Isot. 101, 40-43.

Kossert, K., Marganiec-Gałązka, J., Mougeot, X., Nähle, O.J., 2018. Activity determination of ^{60}Co and the importance of its beta spectrum. Appl. Radiat. Isot. 134, 212-218.

Loidl, M., Rodrigues, M., Censier, B., Kowalski, S., Mougeot, X., Cassette, P., Branger, T., Lacour, D., 2010. First measurement of the beta spectrum of ^{241}Pu with a cryogenic detector. Appl. Radiat. Isot. 68, 1454-1458.

Loidl, M., Rodrigues, M., Le-Bret, C., Mougeot, X., 2014. Beta spectrometry with metallic magnetic calorimeters. Appl. Radiat. Isot. 87, 302-305.

Loidl, M., Beyer, J., Bockhorn, L., Enss, C., Kempf, S., Kossert, K., Mariam, R., Nähle, O., Paulsen, M., Ranitzsch, P., Rodrigues, M., Schmidt, M., 2019. Beta Spectrometry with Metallic Magnetic Calorimeters in the Framework of the European EMPIR project MetroBeta. Appl. Radiat. Isot. 153, 108830.

Los Arcos, J. M., Ortiz, F., 1997. KB: a code to determine the ionization quenching function Q(E) as a function of the kB parameter. Comput. Phys. Commun. 103, 83.

Nähle, O., Kossert, K., 2011. Comparison of the TDCR method and the CIEMAT/NIST method for the activity determination of beta emitting nuclides. LSC2010, Advances in Liquid Scintillation Spectrometry: Proceedings of the 2010 International Conference on Liquid Scintillation Spectrometry, Paris, France, 6-10 September 2010, edited by Philippe Cassette, in Radiocarbon, 2011, the University of Arizona, Tucson, Arizona, USA, ISBN 978-0-9638314-7-7, 313-320.

Nähle, O., Zhao, Q., Wanke, C., Weierganz, M., Kossert, K., 2014. A portable TDCR system. Appl. Radiat. Isot. 87, 249-253.

Mougeot, X., Bisch, C., 2014. Consistent calculation of the screening and exchange effects in allowed β^- transitions. Phys. Rev. A 90, 012501.

Mougeot, X., 2017. BetaShape: a new code for improved analytical calculations of beta spectra. EPJ Web Conf. 146, 12015.

Nähle, O., Kossert, K., Cassette, Ph., 2010. Activity standardization of ^{3}H with the new TDCR system at PTB. Appl. Radiat. Isot. 68, pp. 1534-1536.

Pibida, L., Zimmerman, B.E., King, L., Fitzgerald, R., Bergeron, D.E., Napoli, E., Cessna, J.T., 2020. Determination of the internal pair production branching ratio of ^{90}Y. Appl. Radiat. Isot. 156, 108943.

Rotzinger, H., Linck, M., Burck, A., Rodrigues, M., Loidl, M., Leblanc, E., Fleischmann, L., Fleischmann, A., Enss, C., 2008. Beta spectrometry with magnetic calorimeters. J. Low Temp. Phys. 151, 1087-1093.

Selwyn, R.G., Nicles, R.J., Thomadsen, B.R., DeWerd, L.A., Micka, J.A., 2007. A new internal pair production branching ratio of ^{90}Y: the development of a non-destructive assay for ^{90}Y and ^{90}Sr. Appl. Radiat. Isot. 65, 318–327.

Towner, I.S., Hardy, J.C., 2008. Improved calculation of the isospin-symmetry-breaking corrections to superallowed Fermi β decay. Phys. Rev. C 77, 025501.

Table 1

Recipe for preparation of the $^{90}Sr/^{90}Y$ LS samples. Sample No. 1 is the background sample.

Sample No.	**1**	**2**	**3**	**4**
Ultima Gold™	15 mL	15 mL	15 mL	15 mL
Distilled water	1 mL	0.6 mL	0.6 mL	0.6 mL
CH_3NO_2 (diluted with pseudo-cumene 1:1)	0 µl	0 µl	30 µl	60 µl
Weighed portion of $^{90}Sr/^{90}Y$ solution	0 mg	~400 mg	~400 mg	~400 mg

Table 2

Results of the activity concentration determined with various analysis conditions.

Conditions selected for the analysis	**Activity concentration from CNET in kBq/g**	**Activity concentration from TDCR in kBq/g**	**Relative deviation between both methods**	**Unweighted mean (CNET, TDCR) in kBq/g**	**Relative deviation to final result**
Old approximation with $C(W)=p^2+q^2$, no $SQP(E)$ bias correction, kB= 0.0075 cm/MeV	3.9691	3.9794	0.26%	3.9742	-0.18%
Classical beta spectrum, no $SQP(E)$ bias correction, kB= 0.0075 cm/MeV	3.9738	3.9800	0.16%	3.9769	-0.11%
Classical beta spectrum, with $SQP(E)$ bias correction, kB= 0.0075 cm/MeV	3.9764	3.9800	0.09%	3.9782	-0.08%
Beta spectrum with screening and atomic exchange effect, with $SQP(E)$ bias correction, kB= 0.0075 cm/MeV	3.9806	3.9821	0.04%	**Final result = 3.9813**	0.00%
Beta spectrum with screening and atomic exchange effect, with $SQP(E)$ bias correction, kB= 0.0110 cm/MeV	3.9769	3.98402	0.18%	3.9805	-0.02%

Table 3

Standard uncertainty components assigned to the activity concentration a of a ^{90}Sr solution measured by liquid scintillation counting.

	TDCR	**CNET**
Component	$u(a)/a$ **in %**	$u(a)/a$ **in %**
Statistic (relative standard deviation, 3 samples, number of repetitions per sample ≥ 10)	0.02	0.01
Weighing	0.01	0.01
Dead time	0.05	0.07
Background	0.02	0.02
Adsorption	0.05	0.05
TDCR value	0.02	-
^{3}H standard as tracer	-	0.02
Radionuclide impurities (none detected)	0.05	0.05
Model and decay data (e.g. beta spectrum shape, *kB* parameter etc.)	0.1	0.1
Decay correction	<0.01	<0.01
Square root of the sum of quadratic components	**0.14**	**0.15**

Figure captions

Figure 1: Beta spectra of ^{90}Sr, ^{90}Y and ^{90}Sr/^{90}Y calculated with a new version of the BetaShape program. The calculations were carried out taking the atomic exchange and screening corrections into account (blue dotted line). When ignoring these effects (red dashed line), the result is referred to as the "classical" spectrum. A shape-factor function $C(W)=q^2+p^2$ was used for the spectra denoted by "old approximation" (purple dot-dashed).

Figure 2: LS spectra of ^{90}Sr/^{90}Y recorded with a Wallac 1414 LS counter with a logarithmic amplification (left) and a TriCarb 2800 TR LS counter with a linear amplification (right). Corresponding background spectra have been subtracted.

Figure 3: Left: Bias of the quench-indicating parameter $SQP(E)$ and the ratio of the counting rate of a ^{90}Sr/^{90}Y LS sample and the activity of the external ^{152}Eu standard source. Right: Corresponding bias for the *tSIE* from a TriCarb 2800 TR counter with a ^{133}Ba source as an external standard.

Figure 4: Activity concentration as obtained for the CNET and the TDCR methods as a function of the counting efficiency. The uncertainty bars represent only a statistical component which was calculated as a standard deviation of the mean of several repetition measurements. A shape-factor function $C(W)=q^2+p^2$ was used for data denoted by "old approximation".

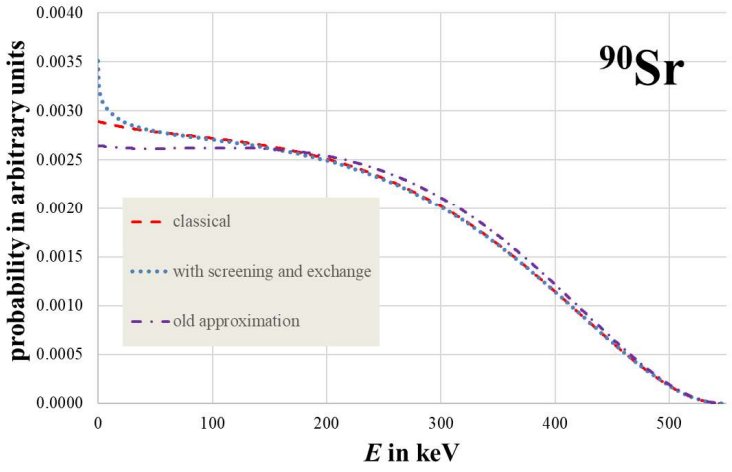
^{90}Sr
probability in arbitrary units
0.0040
0.0035
0.0030
0.0025
0.0020
0.0015
0.0010
0.0005
0.0000
0
100
200
300
400
500
E in keV
classical
with screening and exchange
old approximation

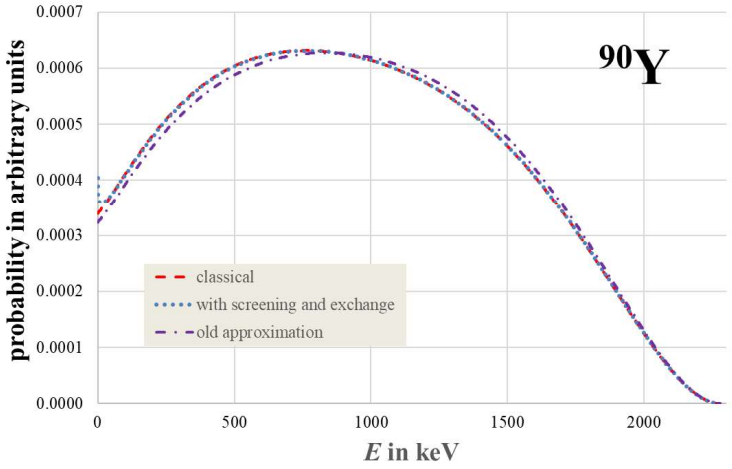
^{90}Y
probability in arbitrary units
0.0007
0.0006
0.0005
0.0004
0.0003
0.0002
0.0001
0.0000
0
500
1000
1500
2000
E in keV
classical
with screening and exchange
old approximation

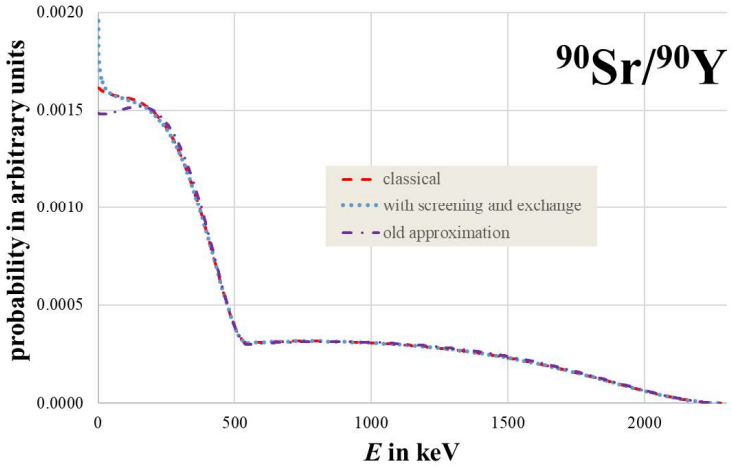
^{90}Sr/^{90}Y
probability in arbitrary units
0.0020
0.0015
0.0010
0.0005
0.0000
0
500
1000
1500
2000
E in keV
classical
with screening and exchange
old approximation

Figure 1

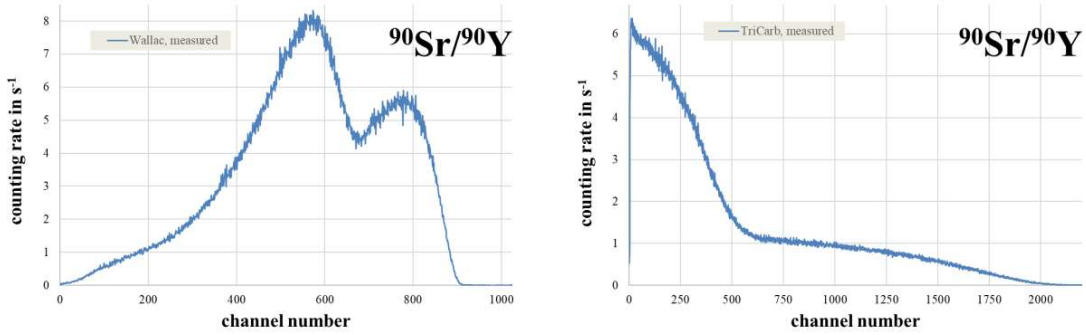

Figure 2

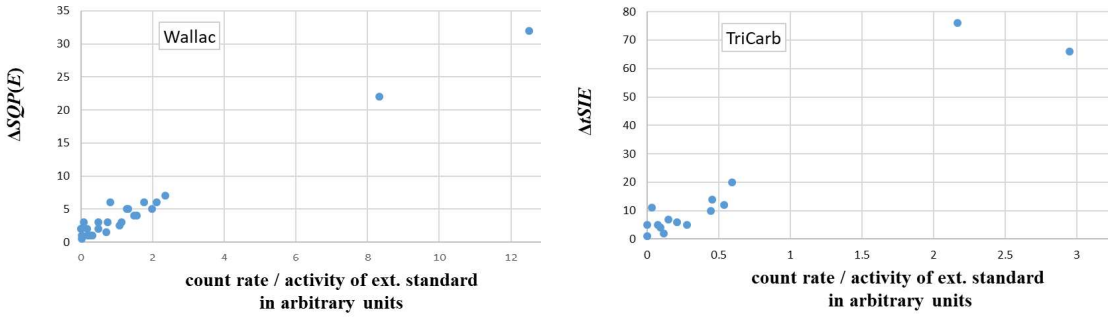

Figure 3

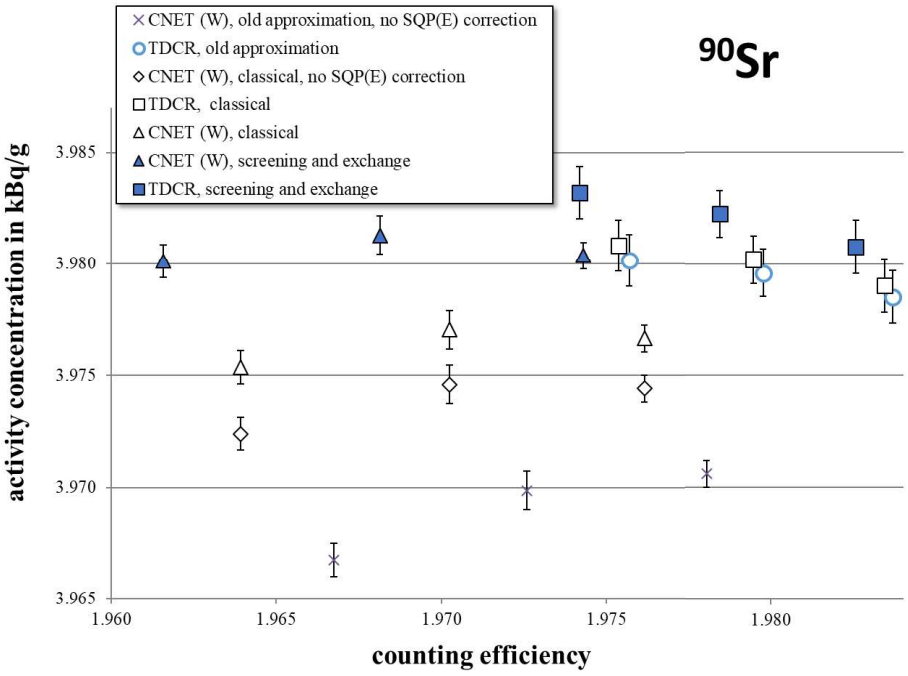
CNET (W), old approximation, no SQP(E) correction
TDCR, old approximation
CNET (W), classical, no SQP(E) correction
TDCR, classical
CNET (W), classical
CNET (W), screening and exchange
TDCR, screening and exchange
90Sr
activity concentration in kBq/g
3.985
3.980
3.975
3.970
3.965
1.960
1.965
1.970
1.975
1.980
counting efficiency

Figure 4